

Modification of Impact Testing Tools for Research of Aluminum Alloys Energy Absorption Profile

Bambang Riyanta^{a*}, Hary Nugroho^a, Budi Nur Rahman^a

^a Department of Mechanical Engineering, Universitas Muhammadiyah Yogyakarta, Yogyakarta, Indonesia
e-mail: bambangriyanta@umy.ac.id*, harynugroho93@gmail.com, budinurrahman@umy.ac.i

Keywords: **ABSTRACT**

Aluminium,
Age hardening,
Impact Test,
ASTM E23-02a,
TIG

One of the most popular materials used in industry is aluminum and its alloys. The aluminum manufacturing process is likely to undergo a welding process. Aluminum can be welded by gas or arc welding, but arc welding is more satisfactory. The welding process on aluminum alloys has the potential to present a situation similar to Age hardening. This research was conducted to dig deeper into the impact of welding on the second phase strengthening mechanism in several series of aluminum alloys using impact test equipment with the addition of a modified digital instrumentation device. Modifications were made to the GOTECH impact test equipment model Charpy impact test 0027 by changing the pendulum and adding a plate to the holder to conform to the ASTM E23-02a standard and adding digital instrumentation tools, including load cells, amplifiers, data acquisition, and power supply. The specimens used were aluminum 5052 and 6061 with variations of base metal and TIG welded V 60°. The results of the modified impact test equipment can display a graph of the impact energy absorption of each specimen. Comparison between the manual calculation of absorbed impact energy and digital calculation of 5052 base metal aluminum specimens has an average deviation of 11,716 J, 5052 welded specimens have an average deviation of 1.341 J, 6061 base metal specimens have an average deviation of 0.729 J, and 6061 welded specimens has a mean of 0.845 J.

1. INTRODUCTION

One of the materials becoming increasingly popular in industries is aluminum and its alloys. Aluminum has a strength exceeding mild steel and is classified as lightweight metal. Aluminum has good corrosion resistance and relatively good ductility in cold conditions, making it applicable in chemistry, construction, electricity, storage equipment, and transportation [1]. Compared to other steels, aluminum has disadvantages in welding. This can be overcome by using arc welding techniques. TIG welding is one of the welding techniques commonly used for aluminum fabrication [2]. The welding process on aluminum alloys can present situations similar to age hardening. The strengthening phenomenon of forming a second phase will likely occur in aluminum alloys post-welding in the weld and heat-affected zones. Based on this, this research is conducted to meet the need for equipment that can be used to further explore the effects of welding on the mechanism of second-phase strengthening in several series of aluminum alloys using impact testing equipment. Charpy impact testing uses a Charpy impact machine equipped with pressure sensors and data acquisition devices to obtain energy absorption recordings during impact according to ASTM E23-02a testing standards [3]. The results of the impact testing data recordings are then compared with manual calculations. Modifying impact testing equipment to adhere to ASTM standards, such as ASTM E23-02a, and integrating digital instrumentation tools like load cells, amplifiers, data acquisition systems, and power supplies significantly enhances the efficacy and reliability of the testing process. Compliance with ASTM standards ensures consistency and comparability of results, while digital instrumentation offers superior accuracy, precision, and efficiency compared to traditional manual methods. The incorporation of digital tools not only automates data collection, reducing the likelihood of human error, but also facilitates faster testing procedures, allowing for more tests to be

conducted within a given timeframe. Moreover, these modifications enhance the equipment's versatility, enabling it to adapt to a wider range of testing requirements and materials, ultimately improving the quality and integrity of impact test results in research and industrial applications

2. METHODS

2.1 Modification of Impact Testing Equipment

GOTECH Charpy impact test model with serial number 0027 does not comply with ASTM E23-02a standards for testing, due to issues like improper calibration, incorrect impact energy range, deviations in geometry, misalignment, and inadequate environmental controls. Additionally, wear and tear or a faulty data acquisition system could also contribute to its non-compliance, necessitating a thorough inspection to identify the specific causes. Thus requiring modification to the impact testing equipment [4]. The holder was modified by adding S4,5C steel plates to mount ASTM standard specimens horizontally. This also affects the pendulum, which cannot swing when mounted. Therefore, it is necessary to make a pendulum suitable for the modified holder [5]. The material used for making the pendulum is S45C steel, while VCN steel is used for the pendulum knife because it is harder than S45C steel, making it suitable for use when impacting test specimens [6-9]. The results of the modifications are shown in Figure 1.



Figure 1. The results of the modifications are as follows: (a) Holder Modification and (b) Pendulum Manufacturing Outcome.

2.2 Digital Instrumentation Equipment

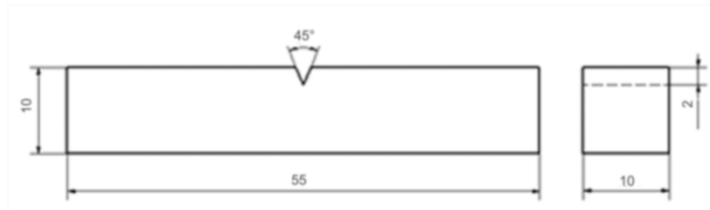
The digital instrumentation equipment used in this research includes a load cell of type S Zemic H3-C3-300kg-3B, Adam 3016 amplifier, Advantech USB-4704 data acquisition device, and S-150-24 power supply model. The circuitry of the digital instrumentation equipment is shown in Figure 1.



Figure 2. Design of base metal specimens (b) Result of specimen fabrication

2.3 Testing Specimen

The test specimens in this study are made of aluminum 5052 and 6061 with dimensions according to ASTM E23-02a standards. Each type of aluminum has a base metal variant and TIG welded V 60° with ER5356 filler. The specimen preparation process uses a CNC machine. The design and results of specimen preparation are shown in Figures 3 and 4 below.

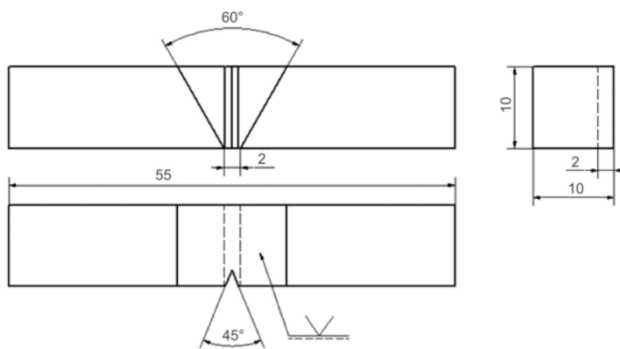


(a)



(b)

Figure 3. Design of base metal specimens (b) Result of specimen fabrication



(a)



(b)

Figure 4. (a) Design of welded specimens (b) Result of specimen fabrication

2.4 Testing Process

After modifying the holder, constructing the pendulum, assembling the digital instrumentation, and preparing the test specimens, the next step is to install the AdvantechDAQ data logger application. This application is associated with the Advantech USB-4704 data acquisition device and serves to record data on the collision process between the pendulum and the test specimen absorbed by the load cell. The AdvantechDAQ data logger application can be seen in Figure 5.

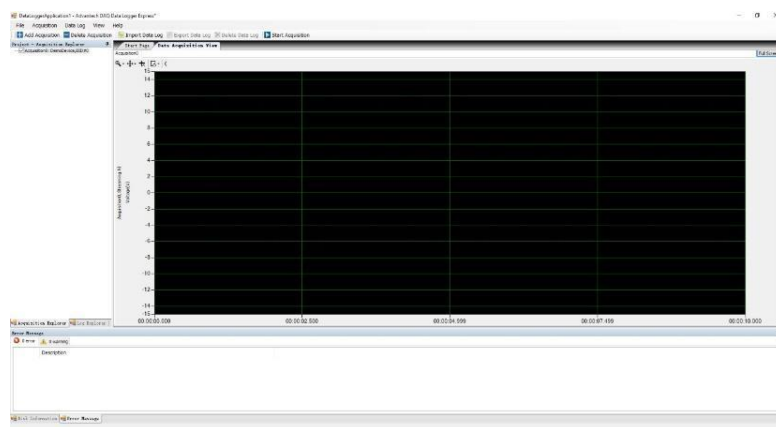


Figure 5. AdvantechDAQ Dashboard

3. RESULT AND DISCUSSION

3.1 Fracture Result

Figures 6 and 7 display the fractured Charpy V-notch specimens made from base metals aluminum 5052 and 6061, including versions with TIG welding at a 60° V-notch. The crack propagation in the base metal, oriented in the longitudinal direction, aligned with the normal impact force. This behavior was due to the granular structure morphology, with elongated grains resulting from the high deformation of the material in the longitudinal direction.

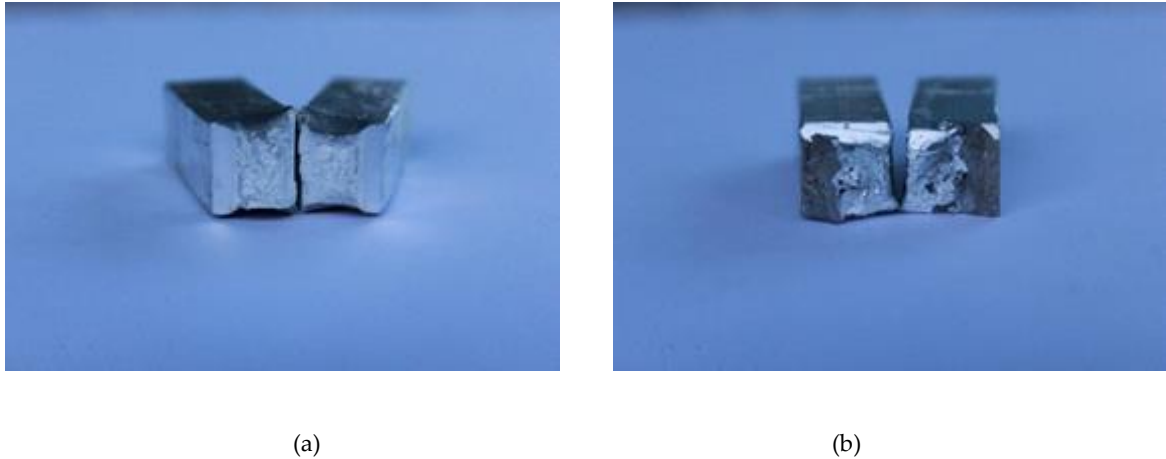


Figure 6. Fracture of aluminum test specimens (a) 5052 base metal (b) 5052 welded

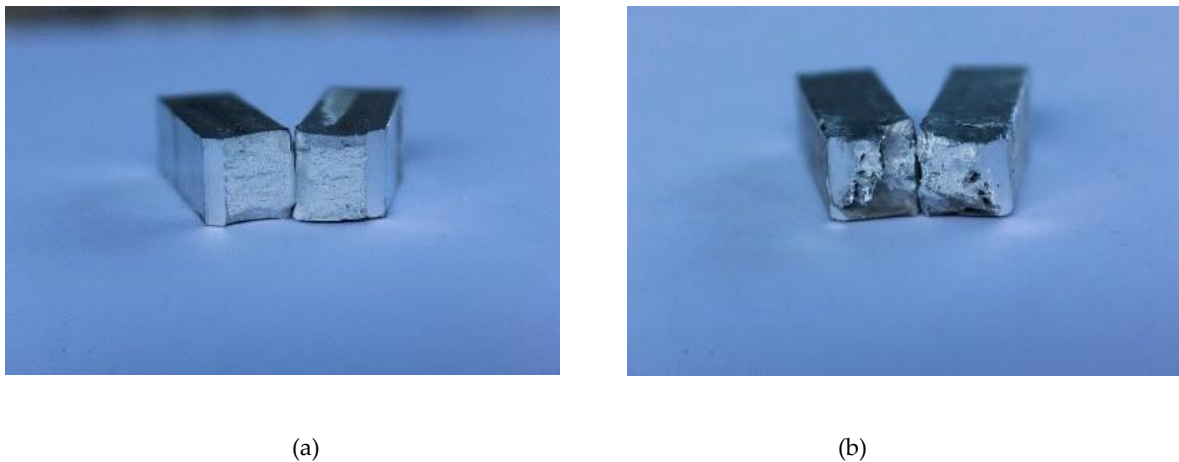
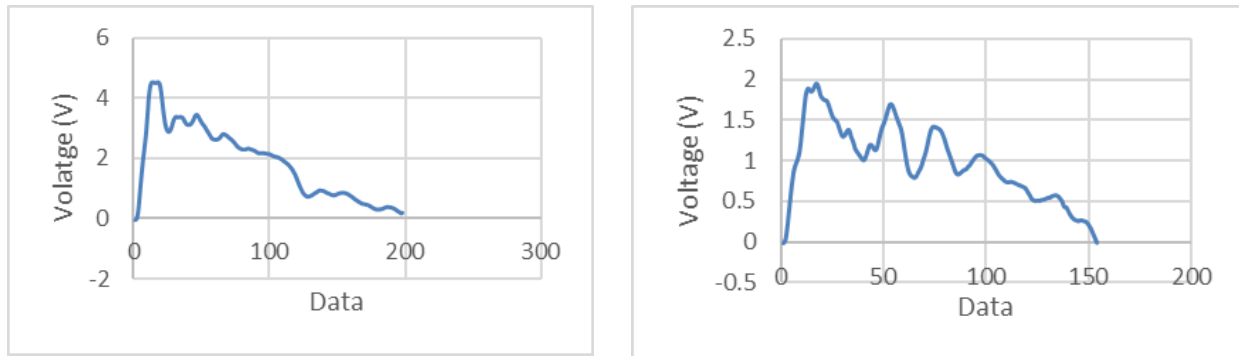


Figure 7. Fracture of aluminum test specimens (a) 6061 base metal (b) 6061 welded

For the weld metal specimens illustrated in Figure 7, the crack propagation exhibits a pattern similar to that of the base metal in the transverse direction. Here, the granular structure is characterized by dendrites with an equiaxed morphology at the weld metal's center. Using an instrumented impact pendulum [10, 11], force versus time curves for 7075-T651 aluminum welds were obtained from standard Charpy-V samples. Analyzing these force-time curves at a constant impact velocity enabled the quantification of fracture energies across different zones. Notably, the heat-affected zone (HAZ) demonstrated a significant improvement in fracture energy (33.6 J) compared to the weld metal (7.88 J) and the base metal (5.37 J and 7.37 J) [11].

3.2 Graph of Each Test Specimen From Recorded Data

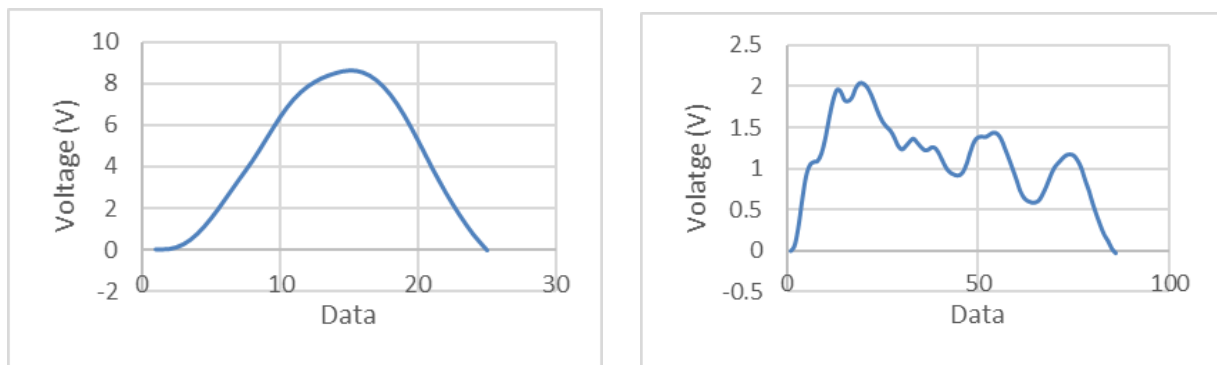
In the data recording of the AdvantechDAQ application for impact testing, the recording interval (dt) or data recording time is set to 0.000025 seconds per data point. The recorded data during one test session has values ranging from tens of thousands to hundreds of thousands, which are then plotted into graphs. The obtained data is then simplified from the rising to the falling of the graph, so that only tens to hundreds of data points are used. The graph of each test specimen is shown in Figure 8 and 9.



(a)

(b)

Figure 8. Simplification of recorded data graph (a) 5052 base metal (b) 5052 welded



(a)

(b)

Figure 9. Simplification of recorded data graph (a) 6061 base metal (b) 6061 welded

3.3 Absorbed Energy and Impact Value

Given the results of the modified impact testing equipment, the pendulum mass is determined to be 5.8 kg, the gravitational acceleration is 9.8 m/s², the distance between the pivot points to the pendulum knife impacting the test specimen is 0.68 m, and the initial pendulum angle is 150°. Therefore, the formula obtained is as follows:

$$E = m \cdot g \cdot r (\cos \beta - \cos \alpha)$$

Impact value = E/A

where,

E = absorbed energy (Joules)

m = mass of the pendulum (kg)

g = gravitational acceleration (m/s²)

r = distance between pivot points to the pendulum knife impacting the test specimen

β = measurement angle (°)

α = initial angle (°)

A = cross-sectional area (m²)

Below are the results of the absorbed energy and impact value from the modification of the GOTECH charpy impact test apparatus for aluminum 5052 and 6061 test specimens with variations in base metal and welding, as shown in Tables 1 and 2.

Table 1. Absorbed energy and impact value (a) 5052 base metal (b) 5052 welded

No	Test Specimen	Measurement Angle	Absorbed Energy	Impact Value
1	5052 Basemetal A	75°	43,476 J	0.543 J/mm ²
2	5052 Basemetal B	68°	47,951 J	0.599 J/mm ²
3	5052 Basemetal C	65°	48,575 J	0.607 J/mm ²
4	5052 Basemetal D	65°	48,575 J	0.607 J/mm ²

(a)

No	Test Specimen	Measurement Angle	Absorbed Energy	Impact Value
1	5052 Welded A	107°	22,172 J	0.277 J/mm ²
2	5052 Welded B	127°	10,212 J	0.128 J/mm ²
3	5052 Welded C	130°	8,628 J	0.108 J/mm ²
4	5052 Welded D	122°	12,991 J	0.154 J/mm ²

(b)

Table 2. Absorbed energy and impact value (a) 6061 base metal (b) 6061 welded

No	Test Specimen	Measurement Angle	Absorbed Energy	Impact Value
1	6061 Basemetal A	115°	17,138 J	0.214 J/mm ²
2	6061 Basemetal B	113°	18,370 J	0.229 J/mm ²
3	6061 Basemetal C	115°	17,138 J	0.221 J/mm ²
4	6061 Basemetal D	117°	15,952 J	0.199 J/mm ²

(a)

No	Test Specimen	Measurement Angle	Absorbed Energy	Impact Value
1	6061 Welded A	119°	14,374 J	0.184 J/mm ²
2	6061 Welded B	115°	18,370 J	0.229 J/mm ²
3	6061 Welded C	127°	10,212 J	0.127 J/mm ²
4	6061 Welded D	120°	14,147 J	0.179 J/mm ²

(b)

3.4 Calibration Result

The calibration process is conducted in several stages. In the first stage, the impact testing results from the acquisition data, which are in voltage values, are converted into P (kg). The specifications of the load cell indicate that 1 volt equals 76.92308 kg. The converted results are compared with the fracture length v (mm), which represents the amount of data used during pendulum contact with the specimen in the form of a graph. The area under the P- v curve is the change in energy or work (W). From the conversion results, it is known that the X-axis represents displacement (mm) and the Y-axis represents force (N) in the form of (kg). Work (Joule) is the result of multiplying displacement (m) by force (N). To determine the area under

the P-v curve, OriginLab software is used. The results of the area under the curve for each test specimen using OriginLab are shown in Figures 3 and 4.

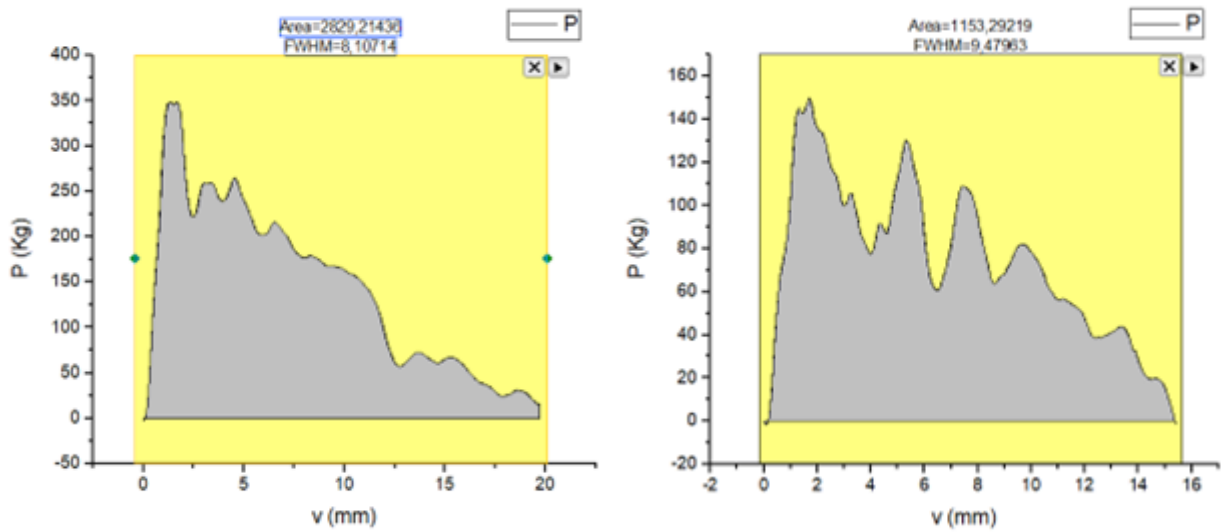


Figure 8. The area under the curve (a) 5052 base metal (b) 5052 welded.

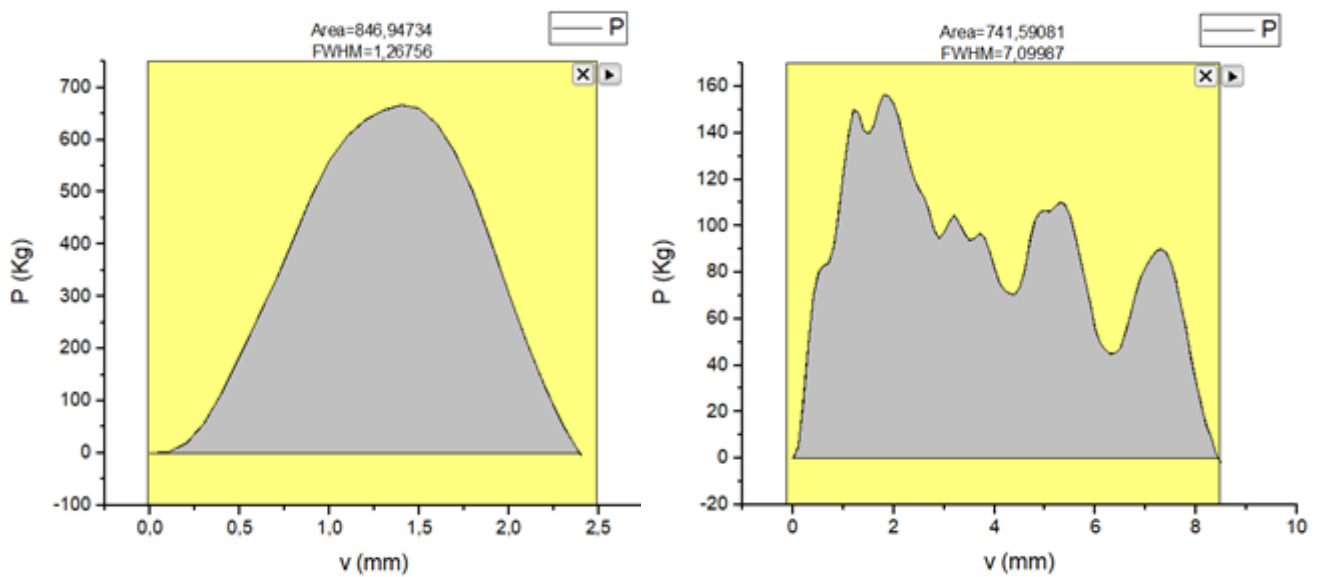


Figure 9. The area under the curve (a) 6061 base metal (b) 6061 welded.

The area values shown on the graph represent the area under the curve. The area under the curve results are in units of kg.mm and then converted into N.m (Joules) to represent absorbed energy. In the impact testing conducted, the load cell is only installed on one side of the holder, so to find the total absorbed energy, it is multiplied by 2. The conversion results are shown in tables 3 and 4.

Table 3. Conversion of the area under the curve (left) 5052 base metal (right) 5052 welded.

No	Test Specimen	The area under the curve	Digital Measurement
1	5052 Basemetal A	27,726 J	55,452 J
2	5052 Basemetal B	29,622 J	59,244 J
3	5052 Basemetal C	30,830 J	61,66 J
4	5052 Basemetal D	29,541 J	59,083 J

(a)

No	Test Specimen	The area under the curve	Digital Measurement
1	5052 Welded A	11,302 J	22,604 J
2	5052 Welded B	6,137 J	12,346 J
3	5052 Welded C	5,064 J	10,128 J
4	5052 Welded D	5,846 J	11,692 J

(b)

Table 4. Conversion of the area under the curve (left) 6061 base metal (right) 6061 welded.

No	Test Specimen	The area under the curve	Digital Measurement
1	6061 Basemetal A	8,300 J	16,6 J
2	6061 Basemetal B	8,499 J	16,998 J
3	6061 Basemetal C	8,399 J	16,798 J
4	6061 Basemetal D	8,309 J	16,618 J

(a)

No	Test Specimen	The area under the curve	Digital Measurement
1	6061 Welded A	7,268 J	14,536 J
2	6061 Welded B	8,187 J	16,374 J
3	6061 Welded C	4,598 J	9,196 J
4	6061 Welded D	7,159 J	14,318 J

(a)

The digital measurement results are compared with the manual measurement of absorbed energy to determine the deviation, thus enabling the determination of whether the modified impact testing equipment is suitable for testing. Below are the comparison results shown in tables 5, 6, 7, and 8.

Table 5. Comparison of manual and digital calculation of absorbed energy for 5052 base metal.

No	Test Specimen	Manual Measurement	Digital Measurement	Deviation
1	5052 Basemetal A	43,476 J	55,452 J	11,976 J
2	5052 Basemetal B	47,951 J	59,244 J	11,293 J
3	5052 Basemetal C	48,575 J	61.662 J	13,085 J
4	5052 Basemetal D	48,575 J	59,083 J	10,508 J

Table 6. Comparison of manual and digital calculation of absorbed energy for 5052 welded.

No	Test Specimen	Manual Measurement	Digital Measurement	Deviation
1	5052 Welded A	22,172 J	22,604 J	0,432 J
2	5052 Welded B	10,212 J	12,346 J	2,134 J
3	5052 Welded C	8,628 J	10,128 J	1,5 J
4	5052 Welded D	12,991 J	11,692 J	1,299 J

Table 7. Comparison of manual and digital calculation of absorbed energy for 6061 base metal.

No	Test Specimen	Manual Measurement	Digital Measurement	Deviation
1	6061 Basemetal A	17,138 J	16,61 J	0,538 J
2	6061 Basemetal B	18,370 J	16,998 J	1,372 J
3	6061 Basemetal C	17,138 J	16,798 J	0,34 J
4	6061 Basemetal D	15,952 J	16,618 J	0,666 J

Table 8. Comparison of manual and digital calculation of absorbed energy for 6061 welded.

No	Test Specimen	Manual Measurement	Digital Measurement	Deviation
1	6061 Welded A	14.374 J	14,536 J	0,198 J
2	6061 Welded B	18.370 J	16,374 J	1,996 J
3	6061 Welded C	10.212 J	9,196 J	1,016 J
4	6061 Welded D	14.147 J	14,318 J	0,171 J

4. CONCLUSION

Based on the results of the modification and impact testing according to ASTM E23-02a using digital instrumentation with aluminum specimens 5052 and 6061 with variations in base metal and welding, the following conclusions can be drawn:

1. The impact toughness of the test specimens can be observed by reading the simplified data recorded in the graph, and the time of specimen fracture can be determined by multiplying the number of data points used on the graph by the recording time of 1 data point (dt).
2. Aluminum 6061 has higher impact toughness compared to aluminum 5052, but aluminum 5052 has higher ductility compared to aluminum 6061.
3. Welding causes a decrease in absorbed energy in both aluminum specimens, and the energy absorption profiles of both aluminum specimens have similarities, possibly due to the use of the same filler.
4. From the results of manual calculation of absorbed energy compared to digital calculation, the specimens of 5052 base metal have an average deviation of 11.716 J, 5052 welded specimens have an average deviation of 1.341 J, 6061 base metal specimens have an average deviation of 0.729 J, and 6061 welded specimens have an average deviation of 0.845 J.
5. Based on these results, 3 out of 4 variations of impact test specimens according to ASTM E23-02a using digital instrumentation have small deviations, indicating that the modification of the impact testing equipment is highly feasible for data collection purposes.

REFERENCES

- [1] N. J. H. Holroyd, G. M. Scamans, R. C. Newman, and A. K. Vasudevan, "Corrosion and Stress Corrosion of Aluminum–Lithium Alloys," *Aluminum-lithium Alloys*, pp. 457–500, 2014, doi: 10.1016/b978-0-12-401698-9.00014-8.
- [2] S. Katoh, "Pulsed TIG Welding of Aluminum," *Encyclopedia of Aluminum and Its Alloys*, 2019, doi: 10.1201/9781351045636-140000431.
- [3] R. R. AMBRIZ, D. JARAMILLO, C. GARCÍA, and F. F. CURIEL, "Fracture energy evaluation on 7075-T651 aluminum alloy welds determined by instrumented impact pendulum," *Transactions of Nonferrous Metals Society of China*, vol. 26, no. 4, pp. 974–983, Apr. 2016, doi: 10.1016/s1003-6326(16)64157-2.
- [4] "Test Methods for Notched Bar Impact Testing of Metallic Materials", doi: 10.1520/e0023-18.
- [5] SHRIWAS, Ankitkumar K.; KALE, Vidyadhar C. Impact of aluminum alloys and microstructures on engineering propertiesreview. *IOSR Journal of Mechanical and Civil Engineering*, 13.3: 16-22 Jun. 2016.
- [6] E. I. Lukin et al., "Effect of the Quenching Temperature on the Structure and Mechanical Properties of Martensitic–Ferritic Corrosion-Resistant Nitrogen-Bearing 08Kh17N2AF Steel," *Russian Metallurgy (Metally)*, vol. 2023, no. 6, pp. 629–637, Jun. 2023, doi: 10.1134/s0036029523060290.
- [7] O. P. Modi, S. Rathod, B. K. Prasad, A. K. Jha, and G. Dixit, "The influence of alumina particle dispersion and test parameters on dry sliding wear behaviour of zinc-based alloy," *Tribology International*, vol. 40, no. 7, pp. 1137–1146, Jul. 2007, doi: 10.1016/j.triboint.2006.11.004.
- [8] B. K. Prasad, O. P. Modi, and A. H. Yegneswaran, "Wear behaviour of zinc-based alloys as influenced by alloy composition, nature of the slurry and traversal distance," *Wear*, vol. 264, no. 11–12, pp. 990–1001, May 2008, doi: 10.1016/j.wear.2007.08.003.
- [9] S. N. Saud, E. Hamzah, T. Asma Abu Bakar, and R. Hosseinian.S, "A Review on Influence of Alloying Elements on the Microstructure and Mechanical Properties of Cu-Al-Ni Shape Memory Alloys," *Jurnal Teknologi*, vol. 64, no. 1, Sep. 2013, doi: 10.11113/jt.v64.1338.
- [10] R. R. AMBRIZ, D. JARAMILLO, C. GARCÍA, and F. F. CURIEL, "Fracture energy evaluation on 7075-T651 aluminum alloy welds determined by instrumented impact pendulum," *Transactions of Nonferrous Metals Society of China*, vol. 26, no. 4, pp. 974–983, Apr. 2016, doi: 10.1016/s1003-6326(16)64157-2.
- [11] RINGER S P, HONO K. Microstructural evolution and age hardening in aluminium alloys: Atom probe field-ion microscopy and transmission electron microscopy studies [J]. *Materials Characterization*, 2000, 44: 101–131.